

SOURCE COMPOSITION OF COSMIC RAYS AT HIGH ENERGY

E. Juliusson, C. J. Cesarsky, M. Meneguzzi, M. Cassé

DPH/EP/ES - Centre d'Etudes Nucléaires de Saclay
B.P. 2 - 91190 Gif-sur-Yvette(France)

The source composition of the cosmic ray is usually calculated at an energy of a few GeV per nucleon. Recent measurements have however indicated that the source composition may be energy dependent. In order to give a quantitative answer to this question we have calculated the source composition at 50 GeV/nucleon using an exponential distribution of pathlengths and in the slab approximation. The results obtained at high energy agree very well with the source composition obtained at lower energies, except the abundance of carbon which is significantly lower than the generally accepted value of low energies.

1. Introduction. A knowledge of the nuclear composition of the cosmic ray sources is of vital importance to the question of the origin of the cosmic rays. In the last decade our knowledge of the composition of the cosmic rays arriving at the earth has greatly increased. At the same time new measurements have been made of some of the important nuclear spallation cross sections. A knowledge of these cross sections, and of the composition enables one to answer important questions about the propagation, and the age of the cosmic rays, and it also allows one to calculate the composition of the cosmic ray source.

The source composition has usually been calculated around 1 GeV/n, since the composition of the arriving cosmic rays is best known in that energy region. Recently however measurements at higher energies have become available, and these have shown that the composition of the arriving cosmic rays depends on their energy. Energy dependent propagation seems to account for most of the observed changes but there have been indications that the carbon/oxygen and the iron/(carbon plus oxygen) ratios change more than can be explained by propagation alone, and that the source composition is thus dependent on energy (Cesarsky and Audouze, 1973, hereinafter referred to as CA).

In order to study the question of possible energy dependence of the cosmic ray composition at the source, we shall in this paper calculate the source composition at 50 GeV/nucleon from measurements reported by Juliusson (1974).

Table I - Fragmentation cross sections in hydrogen

| i | Fragment | i | Be | B | C | N | O | Ne | Mg | F+Na+Al | Si | P-Ca | Sc-Mn | Fe-Ni |
|----|------------|------|-----|-----|-----|-----|-----|-----|-----|---------|-----|------|-------|-------|
| 3 | Lithium | 12.6 | 4.2 | 3.1 | 2.6 | 2.8 | 2.6 | 2.8 | 2.8 | 2.9 | 2.7 | 3.0 | 4.4 | 2.4 |
| 4 | Beryllium | 16.7 | | 2.8 | 1.6 | 1.6 | 1.6 | 1.6 | 1.6 | 1.6 | 1.6 | 1.8 | 2.1 | 2.4 |
| 5 | Boron | 19.7 | | | 7.1 | 3.9 | 3.6 | 2.9 | 2.4 | 2.6 | 2.1 | 1.7 | 1.9 | 1.9 |
| 6 | Carbon | 23.4 | | | | 5.6 | 4.2 | 3.1 | 2.4 | 2.7 | 1.8 | 1.2 | 1.5 | 1.4 |
| 7 | Nitrogen | 24.9 | | | | | 7.0 | 3.9 | 2.9 | 3.2 | 2.2 | 1.4 | 1.4 | 1.3 |
| 8 | Oxygen | 28.9 | | | | | | 6.9 | 5.3 | 6.7 | 4.2 | 2.5 | 2.4 | 2.0 |
| 9 | Fluorine | 32.9 | | | | | | 3.8 | 1.9 | 1.8 | 1.4 | 0.9 | 0.9 | 0.7 |
| 10 | Neon | 33.0 | | | | | | | 7.1 | 8.5 | 5.0 | 3.3 | 2.9 | 2.2 |
| 11 | Sodium | 37.7 | | | | | | | 4.2 | 2.3 | 2.1 | 1.3 | 1.2 | 0.9 |
| 12 | Magnesium | 37.5 | | | | | | | | 10.6 | 8.0 | 4.5 | 3.6 | 2.6 |
| 13 | Aluminium | 42.3 | | | | | | | | | 4.7 | 1.5 | 1.4 | 1.0 |
| 14 | Silicon | 42.8 | | | | | | | | | | 5.8 | 4.5 | 3.2 |
| 15 | Phosphorus | 46.7 | | | | | | | | | | 2.8 | 1.6 | 1.1 |
| 16 | Sulphur | 46.0 | | | | | | | | | | 7.0 | 5.7 | 4.0 |
| 17 | Chlorine | 50.4 | | | | | | | | | | 3.3 | 2.7 | 1.9 |
| 18 | Argon | 49.8 | | | | | | | | | | 8.6 | 6.3 | 4.0 |
| 19 | Potassium | 52.1 | | | | | | | | | | 5.6 | 4.0 | 2.6 |
| 20 | Calcium | 54.6 | | | | | | | | | | | 7.6 | 4.9 |
| 21 | Scandium | 60.9 | | | | | | | | | | | 2.7 | 2.1 |
| 22 | Titanium | 56.9 | | | | | | | | | | | 10.8 | 8.8 |
| 23 | Vanadium | 63.1 | | | | | | | | | | | 5.7 | 3.6 |
| 24 | Chromium | 61.8 | | | | | | | | | | | 10.4 | 11.9 |
| 25 | Manganese | 66.2 | | | | | | | | | | | | 9.2 |
| 26 | Iron | 64.7 | | | | | | | | | | | | 10.0 |
| 27 | Nickel | 70.0 | | | | | | | | | | | | |

2. Propagation. To calculate the composition of the cosmic ray source, we need to know the spallation cross sections σ_{ij} for a nucleus j to break up into a fragment i in a proton collision. The cross sections that we have used are shown in table I. Measured values are used when available (De Lassus and Tobailem, 1972 ; Epherre, 1974 ; Lindström et al. 1975 ; Tobailem and De Lassus, 1975 ; Perron, 1975 ; Regnier, 1975) but otherwise the semiempirical formula of Silberberg and Tsao (1971) is used.

The elemental cross sections σ_{ij} are obtained from the isotopic cross sections $\sigma_{\alpha\beta}$ by summing over different stable isotopes of element i and unstable isotopes that decay into element i during propagation, and averaged over the different isotopes of element j . The total destruction cross sections σ_{α} are calculated from

$$\sigma_{\alpha} = 5.4 (A_{\alpha}^{1/3} - 0.2)^2 \text{ fm}^2 \quad (1)$$

which gives the best fit to the data of Renberg et al. (1972). The cross sections are given in fm^2 ($1 \text{ fm}^2 = 10 \text{ mbarn}$) i. e. area per nucleus. A more natural unit for propagation calculations is however area per unit mass, and we denote by the symbol λ_{ij}^1 the cross sections expressed in cm^2/g .

To calculate the source composition of the cosmic rays in the leaky box model we use the simple relation (Audouze and Cesarsky, 1973)

$$N_i^S = (\lambda_i^{-1} + \lambda^{-1})N_i - \sum \lambda_{ij}^{-1} N_j \quad (2)$$

which follows immediately by setting the production terms equal to the loss terms, as they must be in a steady state. N_i^S and N_j denote the

relative abundances at the source and in the arriving cosmic rays respectively, and λ is the escape length (g/cm^2).

For the slab model and for the atmospheric propagation, the only source of production and loss are the spallation reactions, and we have

$$dN_i/d\lambda = \sum \lambda_{ij}^{-1} N_j - \lambda_i^{-1} N_i \quad (3)$$

where λ is the amount of matter traversed (g/cm^2).

For the cross sections λ_{ij}^{-1} in the atmosphere we have used cross section estimates of Meyer, Westergaard and Cassé, 1975, and we correct the data of all experimenters in the same way. The atmospheric corrections used do not disagree significantly from what one obtains by assuming that the partial cross sections σ_{ij}^1 on one target can be obtained from the partial cross sections σ_{ij} on another target by the relation

$$\sigma_{ij}^1/\sigma_{ij} = (\sigma_i^1/\sigma_i)^{0.5} \quad (4)$$

We note that the propagation equations shown here for the slab (3) and for the leaky box model (2) are extremely simple, and almost trivial to solve. Nevertheless they take correctly into account not only secondary production, but high order production as well.

3. Results. We have taken the results given by Juliusson (1974) for the high energy composition. The data at the lowest energy (24 GeV/n) are not included, and the results at 27 GeV/n are given only half

Table II - Source composition of cosmic rays at 50 GeV/nucleon

| Z | ELEMENT | MEASURED | TOP OF ATM | SLAB MODEL | Exp 1.78 g/cm | 2.5 GeV/n: |
|----|------------|-----------|------------|------------|---------------|------------|
| 3 | Lithium | 124 ± 23 | 53 | - 6 | - 8 ± 23 | - 26 |
| 4 | Beryllium | 65 ± 11 | 24 | - 5 | - 6 ± 11 | - 5 |
| 5 | Boron | 155 ± 16 | 90 | 5 | 6 ± 16 | 6 |
| 6 | Carbon | 857 ± 41 | 788 | 724 | 729 ± 41 | 920 |
| 7 | Nitrogen | 188 ± 17 | 142 | 72 | 77 ± 17 | 118 |
| 8 | Oxygen | 1000 ± 41 | 1900 | 1000 | 1000 ± 41 | 1000 |
| 9 | Fluorine | 18 ± 5 | 2 | - 8 | - 7 ± 5 | - 7 |
| 10 | Neon | 149 ± 16 | 144 | 123 | 121 ± 16 | 119 |
| 11 | Sodium | 35 ± 8 | 22 | 13 | 14 ± 8 | 11 |
| 12 | Magnesium | 182 ± 17 | 181 | 178 | 178 ± 18 | 204 |
| 13 | Aluminium | 28 ± 7 | 20 | 13 | 14 ± 7 | 22 |
| 14 | Silicon | 177 ± 18 | 189 | 205 | 200 ± 19 | 205 |
| 15 | Phosphorus | 8 ± 4 | 4 | 1 | 1 ± 4 | 3 |
| 16 | Sulphur | 32 ± 8 | 30 | 25 | 26 ± 9 | 22 |
| 17 | Chlorine | 5 ± 3 | 1 | - 3 | - 3 ± 3 | - 1 |
| 18 | Argon | 20 ± 6 | 17 | 12 | 12 ± 7 | 3 |
| 19 | Potassium | 6 ± 3 | 3 | - 2 | - 1 ± 3 | 1 |
| 20 | Calcium | 24 ± 7 | 24 | 20 | 20 ± 8 | 21 |
| 21 | Scandium | 6 ± 4 | 3 | 0 | 1 ± 4 | 1 |
| 22 | Titanium | 11 ± 5 | 6 | - 7 | - 4 ± 6 | 2 |
| 23 | Vanadium | 15 ± 6 | 13 | - 9 | 11 ± 7 | - 1 |
| 24 | Chromium | 17 ± 6 | 12 | - 5 | 1 ± 7 | - 7 |
| 25 | Manganese | 17 ± 6 | 14 | 5 | 9 ± 7 | 2 |
| 26 | Iron | 136 ± 17 | 171 | 224 | 212 ± 26 | 218 |
| 28 | Nickel | 11 ± 5 | 14 | 17 | 16 ± 8 | 8 |

weight, since these results are possibly less accurate than the higher energy data, due to background from low energy particles. These data have a representative average energy of about 50 GeV/nucleon. The data used are displayed in Table II which shows the values measured at 6.0 g/cm^2 in the atmosphere, extrapolated to the top of the atmosphere, and to the sources using a slab model, and an exponential pathlength distribution. For most elements, the source value is not very model dependent. The calculated high energy source composition is compared to a value obtained from the same propagation of lower energy data obtained in the same experiment (Juliusson and Meyer, 1975).

We have not yet done an error analysis of the propagation through the atmosphere and through the galaxy and errors due to propagation are not included in Table II. Since the pathlength traversed at high energy is small these propagation errors are in most cases insignificant compared to the statistical errors on the high energy data. At low energy on the other hand the measured abundance errors are in most cases small compared to the propagation errors, and low energy values are shown for comparison only.

The pathlength traversed by the cosmic rays of high energy is significantly shorter than the pathlengths at low energy. Table III gives a summary of the pathlengths obtained from the abundances of the different secondary elements. The pathlength for iron is defined at low

Table III - Cosmic ray pathlengths

| Energy Age | 50 GeV/n | | 25 GeV/n | |
|-----------------------|--|-----------------------------------|--|-----------------------------------|
| | $\text{Be}^{10} \rightarrow \text{B}^{10}$ | $\text{Be}^{10} = \text{Be}^{10}$ | $\text{Be}^{10} \rightarrow \text{B}^{10}$ | $\text{Be}^{10} = \text{Be}^{10}$ |
| λ (Boron) | 1.9 ± 0.3 | 2.1 ± 0.3 | 6.5 ± 0.1 | 7.5 ± 0.1 |
| λ (Beryllium) | 1.4 ± 0.5 | 1.2 ± 0.5 | 5.7 ± 0.2 | 4.2 ± 0.2 |
| λ (Lithium) | 1.5 ± 0.6 | 1.5 ± 0.6 | 5.2 ± 0.2 | 5.2 ± 0.6 |
| λ (iron) | 2.4 ± 0.9 | 2.4 ± 0.9 | 5.8 ± 0.3 | 6.0 ± 0.6 |

energy from the secondary elements scandium to manganese, at high energy by the abundances of scandium to chromium. The errors given are strictly from the errors in the measured abundances of the secondary elements, the cross sections are assumed to be exact. The consistency is better if we assume that Be^{10} has decayed into boron during propagation. The pathlength obtained for boron is consistently larger than that of other secondary components. An intriguing explanation would be that boron was present in the source at the level of a few percent of oxygen. However the cross sections used are probably not accurate enough to give an answer for an eventual boron abundance in the cosmic rays at the source, to better than a few percent, nor even to decide from cosmic ray elemental abundances

whether Be^{10} has decayed or not (Yiou and Raisbeck, 1973). The pathlength used for the source calculation is determined as the one that makes the abundance of boron + beryllium equal to zero. It is thus independent of whether Be^{10} has decayed or not.

The source composition at high energy is quite similar to the one obtained at lower energies. For most elements the difference is smaller than one sigma, ignoring the errors on the low energy source. The iron/oxygen ratio at the source is measured to be the same at high and low energy. We note that the iron spectrum measured by Balasubrahmanyam and Ormes (1973) agrees perfectly with the measurements of Juliusson (1974) both in intensity and spectral slope (Juliusson, 1975). These measurements do therefore not change the conclusion, that a change of the iron to oxygen ratio in the cosmic ray source with energy is at most a small one.

The abundances at the source of the elements magnesium, aluminium, argon and vanadium differ slightly at high and low energy, but we do not consider these differences significant. The only elements for which the high energy source value differ more than two sigma from the value given at low energy are nitrogen and carbon. The difference for nitrogen is small and could be due to statistics. The difference for carbon is larger and the value obtained at high energy is inconsistent with the value given at low energy. It is conceivable that the destruction cross sections for oxygen and carbon deviate significantly from (1), and that the measurements are consistent with a constant C/O ratio at the source for all energies. However the C/O ratio in the cosmic ray source must then be below or close to the value that we obtain at 50 GeV/n for all energies.

In order to study in more detail the source abundances of carbon, nitrogen and iron at different energies, we have calculated the source composition for individual datapoints from Juliusson (1974), Smith et al. (1973) and Webber (1973). Figure 1 shows the pathlength needed to make the beryllium plus boron abundances in the source equal to zero. The line shown is the best powerlaw fit to the data in Table II.

$$\lambda \propto E_T^{-0.49 \pm 0.05}$$

Propagation errors, which are not included in fig. 1, could change the pathlength, but they do not affect the significance of its energy dependence. Whether the decrease in pathlength continues beyond

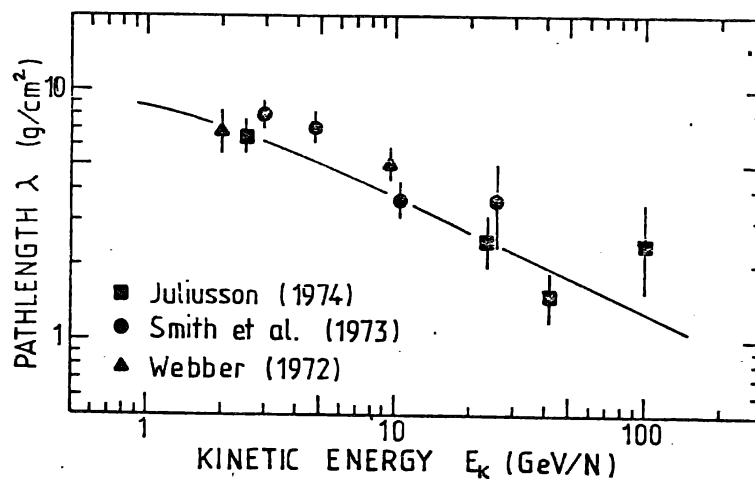


Fig. 1. Pathlength traversed by the cosmic rays

50 GeV/nucleon, cannot be answered by the present data. For the calculations in this paper we include 35% helium (per mass) in the interstellar medium. That does not significantly change the source composition but results in an increase of the pathlengths by about 15%.

Fig. 2 shows the measured source abundances of carbon/oxygen, nitrogen/oxygen and the iron group (Fe + Ni) as a function of energy. The individual datapoints support the conclusion reached from Table II, that the C/O and N/O ratios vary with energy while Fe/O is constant. The errors on the low energy points are unrealistic however since they do not include propagation errors.

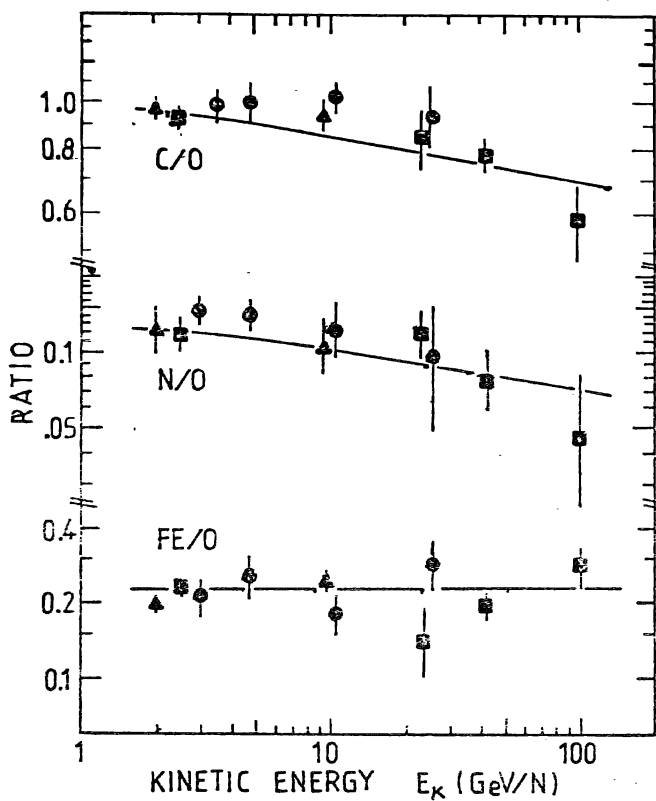


Fig. 2. Relative source abundances of the cosmic rays.

The lines in fig. 2 are a best powerlaw fit to the data in Table II. They correspond to a difference in spectral index of 0.08 between carbon and oxygen and a difference of 0.16 between nitrogen and oxygen.

We thank J.P. Meyer for many valuable discussions and P. Goret for assistance in calculating the atmospheric corrections.

References

- Audouze J. and Cesarsky C.J., 1973, *Nature Phys. Science*, Vol. 241, N°109, p. 98
 Cesarsky C.J. and Audouze J., 1974, *Astron. and Astroph.* 30, 119
 De Lassus C. Tobailem J., 1972, Report CEA-N, 1966 (2) Saclay
 Epherre M., 1974, Private communication
 Juliusson E., 1974, *Ap. J.* 191
 Juliusson E., 1975, paper, this conference EA 1-1
 Juliusson E. and P. Meyer, 1975, paper this conference OA 6-6
 Lindstrom P.J., Greiner Q.E., Heckman H.H., Cork B., Bieser F.S., 1975, Preprint Lawrence Berkeley Laboratory
 Meyer J.P., Westergaard N., Cassé M., 1975, to be published
 Ferron C., 1975, thesis, Orsay, France
 Regner, 1975, Private communication
 Renberg P.U., Measday D.F., Pepin M., Schwaller P., Favies B. and Richard-Serre C., 1972, *Nucl. Phys. A* 183, 81
 Silberberg R. and Tsao CH., 1971, Preprint Naval Research Laboratory
 Smith L.H., Buffington A., Smoot G.F., Alvarez L.W. and Wahliq W.A., 1973 *Ap. J.* 180, 987
 Tobailem J., De Lassus Ch., Leveque J., 1971, Report CEA-N, 1966 (1) Saclay
 Tobailem J., De Lassus Ch., 1975, Private communication
 Webber, 1972, Preprint, "Cosmic ray charge measurements", A 1972, Summary.
 Yion F. and Raisbeck G., 13th Int. Conf. Denver, 1973, 1, 494